



Superstructure-foundation interaction in multi-objective pile group optimization considering settlement response

Journal:	<i>Canadian Geotechnical Journal</i>
Manuscript ID	cgj-2016-0498.R1
Manuscript Type:	Article
Date Submitted by the Author:	22-Jan-2017
Complete List of Authors:	Leung, Yat Fai; The Hong Kong Polytechnic University, Civil and Environmental Eng Klar, Assaf; Technion - Israel Institute of Technology Soga, Kenichi; University of California Berkeley Hoult, Neil; Queen's University
Keyword:	Piled foundation, Superstructure stiffness, Matrix condensation method, Optimization analysis

SCHOLARONE™
Manuscripts

Superstructure-foundation interaction in multi-objective pile group optimization considering settlement response

Y.F. Leung^{1*}, A. Klar², K. Soga³, and N.A. Hoult⁴

¹Department of Civil and Environmental Engineering, The Hong Kong Polytechnic University

²Faculty of Civil and Environmental Engineering, Technion–Israel Institute of Technology

³Department of Civil and Environmental Engineering, University of California, Berkeley

⁴Department of Civil Engineering, Queen’s University

*Corresponding author, email address: andy.yf.leung@polyu.edu.hk

Abstract

The full potential of pile optimization has not been realized as the interactions between superstructures and foundations, and the relationships between material usage and foundation performance are rarely investigated. This paper introduces an analysis and optimization approach for pile group and piled raft foundations, which allows coupling of superstructure stiffness with the foundation model, through a condensed matrix representing the flexural characteristics of the superstructure. This coupled approach is implemented within a multi-objective optimization algorithm, capable of providing a series of optimized pile configurations at various amounts of material. The approach is illustrated through two case studies. The first case involves evaluation of the coupled superstructure-foundation analyses against field measurements of a piled raft-supported building in London, U.K. The potential benefits of pile optimization are also demonstrated through re-analyses of the foundation by the proposed optimization approach. In the second case, the effects of a soft storey on the superstructure-foundation interactions are investigated. These cases demonstrate the importance of properly considering the superstructure effects, especially when the building consists of stiff components such as concrete shear walls. The proposed approach also allows engineers to make informed decisions on the foundation design, depending on the specific project finances and performance requirements.

Keywords :Piled foundation, Superstructure stiffness, Matrix condensation method, Optimization analysis

1 Introduction

2 Foundation optimization presents opportunities to enhance engineering performance
3 by accounting for specific project conditions, with potential savings in material con-
4 sumption and costs. Earlier studies on the topic include Chow and Thevendran (1987),
5 Truman and Hoback (1992), Horikoshi and Randolph (1998), Valliappan et al. (1999),
6 Kim et al. (2001), Reul and Randolph (2004), and Leung et al. (2010b), etc. While
7 the general features of optimal pile group designs have been discussed by some of these
8 studies, it is difficult to derive an efficient technique to obtain optimum designs for
9 various site conditions, considering the complexity of soil-pile interaction effects and
10 potential stiffness contributions from the adjoining superstructure.

11 Due to the discrete nature of some design variables (e.g., number of piles and their
12 locations), a mathematically continuous and differentiable function may not be formu-
13 lated easily, and hence gradient-based optimization techniques are not always appropri-
14 ate for such problems. To address this issue, Kim et al. (2002) applied an evolutionary
15 algorithm, known as the Genetic Algorithm, to determine optimal pile locations in a
16 piled raft design. Most evolutionary algorithms involve creation of an initial random
17 population of candidate solutions (e.g. pile configurations), each evaluated by an objec-
18 tive function (e.g. foundation analysis model) which determines its survivability. The
19 weak candidates (configurations that result in large settlements) are discarded and re-
20 placed by new members of the population, generated by combining the characteristics
21 of ‘strong’ candidates. During this iterative process, the population gradually evolves
22 based on the selection criteria. The application of evolutionary algorithms to foundation
23 optimization has also been discussed by Ng et al. (2005), Chan et al. (2009), Hwang et al.
24 (2011), Liu et al. (2012), etc. In this study, the significance of superstructure stiffness
25 on foundation optimization will be investigated, while the relationship between mate-

26 rial usage and optimal system performance will be revealed through multi-objective
27 optimization analyses.

28 The optimization process is essentially driven by the objective function and selec-
29 tion criteria. For large pile groups, the critical design criteria are often associated with
30 the differential settlements or distortions. Evaluations of such are significantly affected
31 by features of the superstructure, yet the superstructure-foundation interactions are
32 not rigorously considered in many pile group analyses, let alone their optimizations.
33 Existing approaches to characterize such interactions include approximating the super-
34 structure as beams with an equivalent stiffness (e.g. Meyerhof 1953; Sommer 1965) in
35 the geotechnical model, or simulating the piles as ‘spring constants’ (e.g. Miyahara and
36 Ergatoudis 1976) in the structure model. These, however, oversimplify the mechanism
37 of interactions between superstructure, piles and the soil. Inaccurate modeling of such
38 interaction effects in the objective function will also lead to unrealistic optimization
39 results. Another common approach to evaluate the interactions involves iterative re-
40 finements of structural and geotechnical calculations (e.g. Chamecki 1956; Weigel et al.
41 1989). However, an iterative process increases the time and effort involved in a single
42 foundation analysis, and the problem is exacerbated when optimization of pile layouts
43 is required.

44 This paper introduces an analysis and optimization tool for piled foundations, which
45 also enables efficient coupling of the superstructure stiffness. A multi-objective opti-
46 mization technique is adopted to produce a series of optimized solutions at different
47 amounts of material usage, thus providing the designer with a range of options accord-
48 ing to the financial setup of the project. The analysis model (objective function) is
49 first validated through a case study in London, U.K., where the potential benefits of
50 foundation optimization are also demonstrated. A second case is then presented, which
51 consists of a building with significant differences in stiffness across the storeys – a com-

52 mon practice for buildings with an atrium floor design. Through analyses of the two
53 cases, this study will illustrate the importance of superstructure-foundation interaction
54 in pile group modeling and optimization strategies. Preliminary studies on some of the
55 components have been discussed in Leung et al. (2010a) and Leung et al. (2011), with
56 illustrations on simple hypothetical scenarios. In the current study, however, the ex-
57 tended approach is evaluated with real building layouts, where the influence of various
58 structural forms are discussed in detail.

59 **Coupled superstructure-foundation modeling approach**

60 **Condensed superstructure stiffness matrix**

61 The characteristics of the superstructure can play a crucial role in the overall structure
62 and foundation performance (Small 2001; Poulos 2016), and the main objective of this
63 study is to investigate such effects in pile optimization considerations. In the current
64 study, the superstructure stiffness is incorporated into the piled raft foundation anal-
65 yses through the matrix condensation method. In many building projects, structural
66 engineers construct building models for design purposes using finite element packages.
67 The complete structure model will consist of all the members in the building structure.
68 Using these models, a ‘condensed’ structure matrix, denoted as \mathbf{K}^s in the current work,
69 can be generated by applying a unit displacement at each column in sequence, thus
70 extracting the reaction forces at all other supports due to the unit displacement. For
71 example, the component $\mathbf{K}_{i,j}^s$ in the condensed matrix represents the reaction force at
72 support i due to a unit displacement applied at support j (Fig. 1a). Unlike the complete
73 structural stiffness matrix, the condensed structure matrix is fully populated. For one
74 degree of freedom, the size of condensed matrix will be $n \times n$, where n is the number
75 of columns or supports connecting the superstructure and the foundation. In many

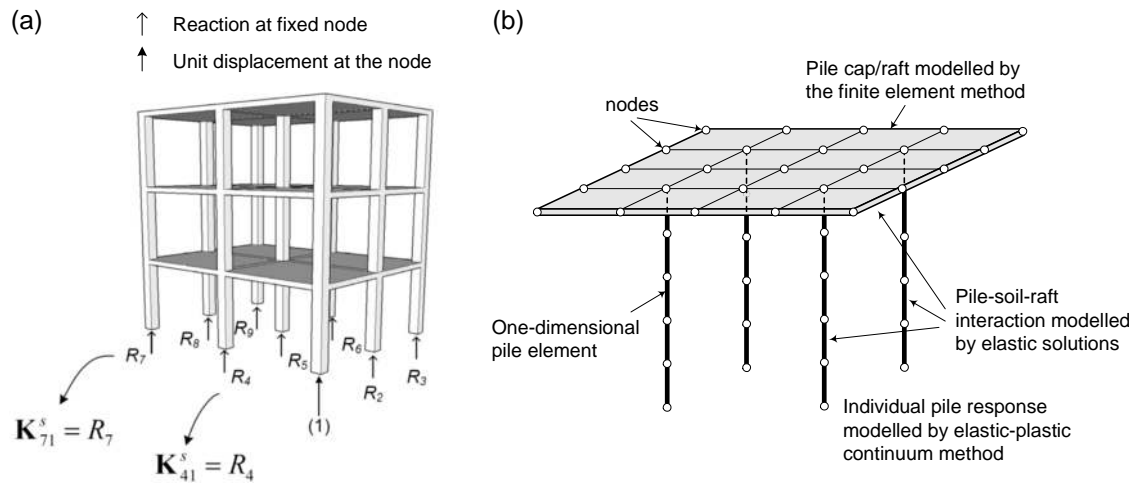


Figure 1: (a) Structure condensation process using finite element simulation, considering vertical load-settlement response (Leung et al. 2010a); (b) Schematic representation of piled raft model

76 cases, the superstructure may consist of continuous shear walls, and the associated
 77 $\mathbf{K}_{i,j}^s$ components can be obtained by incorporating a number of discrete supports along
 78 the wall in the finite element analyses. Poulos (1975) and Brown and Yu (1986) had
 79 discussed the formulation of such a matrix, but the subsequent analyses were focused
 80 on simple frame structures with assumptions of linear-elastic soil behavior. A similar
 81 sub-structuring technique had also been applied previously to replace the foundation by
 82 a condensed matrix, with the drawback of requiring an iterative solution process to ac-
 83 count for nonlinear foundation response. In the current study, the matrix condensation
 84 method will be applied to represent the superstructure model, coupled with nonlinear
 85 analyses and optimizations of large pile groups and piled rafts.

86 The condensed structure matrix can be obtained by structural engineers using most
 87 structural finite element programs. To cover all load cases, the condensation process
 88 should also include horizontal and moment response (assuming the decision is made to
 89 detail the column-foundation connection to transfer moments), with a total of 6 degrees
 90 of freedom for each support (i.e. $6n \times 6n$ condensed matrix). This study will focus on the

91 vertical load-settlement response with an $n \times n$ condensed matrix, while optimization
92 of pile configurations will be performed to minimize vertical differential settlements. As
93 the construction of structural finite element models has become increasingly common in
94 building projects, the additional effort required to obtain the condensed matrix, which
95 involves n analyses with prescribed unit displacements at the supports, is minimal. In
96 fact, even if all 6 degrees of freedom are considered, the computational demands are not
97 substantial, although manually handling the analysis may take more time before such
98 operations are automated in commercial finite element programs. Meanwhile, coupling
99 this condensed structure matrix into pile group analyses leads to more realistic modeling
100 of the combined superstructure and foundation behavior, and eliminates the need for
101 assumptions of Winkler spring constants or subgrade moduli, which cannot represent
102 the behavior of soil continuum realistically.

103 A major assumption of the current approach is that the superstructure behaves
104 in a linear-elastic manner. This is a more reasonable assumption in steel structures
105 than in reinforced concrete buildings. However, this assumption is considered to be
106 appropriate at working load levels for both steel and reinforced concrete buildings as
107 the elastic modulus of concrete can be assumed to be linear at these levels. As will
108 be discussed in later sections, the largest contribution to the stiffness comes from the
109 shear walls, which will remain largely uncracked at working load levels, thus justifying
110 the above assumption. Also, in a superstructure-foundation interaction problem, most
111 of the nonlinearity will be contributed by the foundation response that arises from the
112 nonlinear behavior at the soil-pile interface, and this will be discussed in the formulation
113 of pile group analysis method in the next section.

114 It is worth noting that the actual superstructure stiffness changes as the building is
115 being constructed. If the \mathbf{K}^s matrix is developed based on the full building model, the
116 foundation system will not experience its full stiffening effects when the building is still

117 under construction. Meanwhile, the structural loads also increase with the construction
118 process, leading to progressive changes in both load and stiffness that interact with the
119 foundation. Brown and Yu (1986) stated that the interactions between a steel-framed
120 structure and its raft foundation will be affected by assumptions of the loading sequence,
121 i.e., whether the load is applied ‘instantaneously’ or ‘progressively’ in the model. In
122 their settlement analyses, the discrepancies between the two models reduce as the raft
123 becomes stiffer (increase in raft-to-soil stiffness ratio). The influence of loading sequence
124 for a stiff structure on piled foundations will be assessed in a subsequent case study.

125 **Pile group/piled raft analysis method**

126 Fig. 1b shows the schematic diagram of the analysis model for pile groups and piled
127 rafts. The raft (or pile cap) and the piles are discretised into segments specified by nodes,
128 with the raft modelled as a thin plate using four-node rectangular elements. The nodal
129 force vector and raft stiffness matrix are evaluated through the finite element method
130 (Zienkiewicz and Taylor 2005). Interactions between the soil, raft and piles are evaluated
131 based on elastic solutions, such as the Mindlin (1936) solution for homogeneous half
132 space, or the Chan et al. (1974) solution for two-layered profiles, e.g., in cases where
133 the bedrock is close to the pile tip level. Where the soil modulus increases linearly with
134 depth (‘Gibson soil’), the average Young’s modulus of the two corresponding elements
135 is used to evaluate the interaction effects, as suggested by Poulos (1979).

136 To model soil nonlinearity, a slip element (plastic slider) is incorporated into the
137 continuum solution to limit the contact stresses between the soil and pile shafts and
138 bases, and between the raft and the soil underneath. Formulation of this foundation
139 analysis method has been described in detail by Leung et al. (2010b), and only the
140 extensions to include superstructure effects are detailed herein. Considering the pile

141 group/piled raft system, the soil-structure interaction can be described by:

$$(\mathbf{K}^p + \mathbf{K}^r) \mathbf{u} = \mathbf{p}^s + \mathbf{p}^g \quad (1)$$

142 where \mathbf{K}^p is the structural stiffness matrix of the pile group, \mathbf{K}^r is the raft stiffness
 143 matrix, \mathbf{u} is the vector of raft and pile displacements at the nodes, \mathbf{p}^s is the interaction
 144 force of the superstructure acting on the foundation, \mathbf{p}^g is the ground reaction force
 145 acting on the pile and raft elements. For the superstructure to be in equilibrium, the
 146 following can be derived:

$$\mathbf{K}^s \mathbf{u} = \mathbf{p}^{fdn} + \mathbf{p}^w \quad (2)$$

147 where \mathbf{K}^s is the condensed superstructure stiffness matrix mentioned earlier, \mathbf{u} is the
 148 vector of column displacements, which is equal to the displacements at the correspond-
 149 ing foundation nodes connected to the columns. \mathbf{p}^{fdn} is the interaction force of the
 150 foundation acting on the superstructure, and \mathbf{p}^w is the loading due to the self-weight
 151 and live loads acting on the structure. It should be noted that the superstructure-
 152 foundation interaction forces are considered in \mathbf{p}^{fdn} , and therefore \mathbf{p}^w represents the
 153 gravity loads assuming no interaction with the foundation (i.e. fixed foundations). This
 154 can be obtained from the support reactions assuming zero displacements at the sup-
 155 ports in the superstructure model. Also, since \mathbf{p}^s and \mathbf{p}^{fdn} are action-reaction forces,
 156 they have equal magnitude but opposite signs:

$$\mathbf{p}^s = -\mathbf{p}^{fdn} = \mathbf{p}^w - \mathbf{K}^s \mathbf{u} \quad (3)$$

157 The reaction \mathbf{p}^s can be interpreted as the superposition of two loads, one being the
 158 gravity load reactions using the fixed foundation system and the other being due to
 159 the differential settlements of the superstructure. It should be noted that $\mathbf{K}^s \mathbf{u}$ is

160 only influenced by relative displacements between the supports, and is independent of
 161 the rigid body settlement of the whole structure. Substituting Eq. (3) into (1), and
 162 rearranging, results in:

$$(\mathbf{K}^p + \mathbf{K}^r + \mathbf{K}^s) \mathbf{u} = \mathbf{p}^w + \mathbf{p}^g \quad (4)$$

163 Eq. (4) is the governing equation of the coupled superstructure-foundation behavior.
 164 To model soil nonlinearity using slip elements, the procedures described in Leung et al.
 165 (2010b) are adopted, and Eq. (4) can be rewritten as:

$$\begin{aligned} (\mathbf{K}^p + \mathbf{K}^r + \mathbf{K}^s + \mathbf{K}^*) \mathbf{u} &= \mathbf{p}^w + \mathbf{K}^* \boldsymbol{\lambda}^* \langle (\mathbf{K}^p + \mathbf{K}^r) \mathbf{u} \rangle + \mathbf{K}^* \mathbf{u}^{ip} \\ \langle (\mathbf{K}^p + \mathbf{K}^r) \mathbf{u} \rangle_i &= \min [(\mathbf{K}^p + \mathbf{K}^r) \mathbf{u}, f_{lim}] \end{aligned} \quad (5)$$

166 where \mathbf{K}^* is defined as the local soil stiffness matrix and is diagonal, $\boldsymbol{\lambda}^*$ is the soil
 167 flexibility matrix without the main diagonal, f_{lim} is the limit force at the raft and pile
 168 nodes, and \mathbf{u}^{ip} represents the plastic interface displacements associated with the nodes.
 169 The soil-pile shaft contact force and soil-raft contact force are limited by different values
 170 of f_{lim} . Essentially, Eq. (5) introduces a plastic slider into the continuum solution, and
 171 an iterative procedure (Klar et al. 2007) is necessary to obtain the plastic displacements
 172 (\mathbf{u}^{ip}) at the soil-pile interface to represent the nonlinear foundation response. This
 173 elastic-plastic piled raft analysis approach (without considering the superstructure) has
 174 been shown to produce reasonable representations of nonlinear pile group and piled
 175 raft response (e.g. Poulos 1989; Guo and Randolph 1997; Leung et al. 2010c). It has
 176 also been validated against numerical analyses by Poulos et al. (1997) and several
 177 case histories in Europe (Katzenbach et al. 2000; Reul and Randolph 2003), details of
 178 which can be found in Leung (2010). In cases of complex subsurface stratigraphies,
 179 it is possible to incorporate the ‘load transfer’ approach into the current framework.
 180 This can be achieved by modifying the soil flexibility matrix in Eq. (5) using different

181 nonlinear load transfer relationships for the associated soil layers.

182 Once the foundation settlements are determined, the corresponding settlements at
183 column supports can be input into the superstructure model to obtain distribution of
184 forces and moments in the structural members. This is different than most existing
185 software packages that directly simulate the pile response as independent springs at
186 column supports of the superstructure model, without considering the interaction effects
187 among piles in the soil continuum. This drawback recently prompted Comodromos et al.
188 (2016) to propose a method allowing for interaction among piles and the raft under
189 combined loadings. The proposed approach in this study rigorously considers such pile-
190 to-pile interaction effects, which can only be achieved otherwise by a complete three-
191 dimensional finite element model consisting of the superstructure, foundation piles, and
192 the entire soil domain. Meanwhile, the adopted coupling method allows a much faster
193 simulation of all these components than the complete finite element model, and enables
194 optimization analyses to be performed efficiently. In subsequent sections, this coupled
195 superstructure-foundation analysis approach will be validated against measurements
196 of a piled raft-supported building in London, U.K. Integration of this approach with
197 optimization techniques will also be illustrated.

198 **Multi-objective optimization algorithm**

199 An efficient optimization algorithm can lead to savings in materials and improvements
200 in foundation performance. Most previous studies on foundation optimization consid-
201 ered ‘single-objective optimization’, where the goal was either minimizing material costs
202 under a tolerable performance level, or achieving the best performance with a certain
203 amount of material (e.g. Kim et al. 2001; Chan et al. 2009). The two criteria in (min-
204 imizing) material usage and (maximizing) foundation performance were, however, not
205 considered simultaneously. Also, the influence of superstructure was either ignored or

206 grossly simplified in most previous works.

207 In the current study, the condensed superstructure stiffness (\mathbf{K}^s) is included into the
 208 foundation model. This becomes the objective function integrated into a multi-objective
 209 optimization algorithm, which is developed to obtain a range of optimized foundation
 210 solutions at different amounts of material usage. The technique is an extension of the
 211 Differential Evolution (DE) algorithm proposed by Storn and Price (1997) for search
 212 and optimization purposes, and is conceptually similar to other evolutionary algorithms.
 213 Besides demonstrating the potential benefits of foundation optimization, the study also
 214 aims to reveal the full stiffening effects of the superstructure as the holistic foundation-
 215 structure system performance is optimized.

216 Differential evolution

217 In the DE optimization process, a population of NP candidate solutions is first gener-
 218 ated randomly. The candidate solutions are expressed as vectors of variables (known as
 219 trial vectors, \mathbf{x}_i) in the optimization problem. The algorithm then explores the search
 220 space by vector difference of the various candidate solutions. At each iteration (or
 221 ‘generation’), ‘mutant vectors’ (\mathbf{v}_i) are formed by linear interpolation or extrapolation
 222 of trial vectors randomly selected from the population. A new generation of trial vec-
 223 tors (\mathbf{y}_i) is then formed by the ‘crossover’ process, whereby the components of mutant
 224 vectors are mixed with those of the trial vectors in the previous generation. The DE
 225 optimization process can be represented by the following equations (Storn and Price
 226 1997):

$$\mathbf{v}_{i,G+1} = \mathbf{x}_{r1,G} + F(\mathbf{x}_{r2,G} - \mathbf{x}_{r3,G}) \quad (6)$$

227 where $\mathbf{v}_{i,G+1}$ is the mutant vector in generation $G + 1$, formed by interpolation of three
 228 randomly selected trial vectors from the previous generation G . F is an amplification fac-
 229 tor of the differential variation between two trial vectors $\mathbf{x}_{r2,G}$ and $\mathbf{x}_{r3,G}$. The crossover

230 process is then represented by:

$$\begin{aligned}
 \mathbf{y}_{i,G+1} &= \{y_{1i,G+1}, y_{2i,G+1}, \dots, y_{Di,G+1}\}^T \\
 y_{ji,G+1} &= \begin{cases} v_{ji,G+1} & \text{if } randb(j) \leq CR \text{ or } j = rnbr(i) \\ x_{ji,G} & \text{if } randb(j) > CR \text{ and } j \neq rnbr(i) \end{cases}, j = 1, 2, \dots, D \quad (7)
 \end{aligned}$$

231 where $y_{ji,G+1}$ is the j^{th} component of the new trial vector, which, like \mathbf{x}_i and \mathbf{v}_i , has D
 232 components. CR is a crossover constant chosen by the user and $randb(j)$ are random
 233 numbers to be compared with CR to decide values of $y_{ji,G+1}$. Another random index,
 234 $rnbr(i)$, which is a random integer between 1 to D , is introduced to ensure $\mathbf{y}_{i,G+1}$ has
 235 at least one component of $\mathbf{v}_{i,G+1}$.

236 Fitness of $\mathbf{x}_{i,G}$ (parent, in generation G) and $\mathbf{y}_{i,G+1}$ (child, in generation $G +$
 237 1) are evaluated and compared through an objective function, which is the coupled
 238 superstructure-foundation analysis in the current study. The fitness (e.g., foundation
 239 settlement) determines the survivability of the particular solution – the fitter solutions
 240 stay in the population, while the weaker ones will be discarded. The comparisons are
 241 performed for each parent-child pair (i from 1 to NP), and the procedures are iterated
 242 until the population converges to a global optimum solution.

243 Pareto Optimality

244 It is a common perception that reducing material usage and improving foundation
 245 performance are two conflicting design criteria: more foundation material often leads
 246 to better overall foundation performance, but this is limited by the financial implications
 247 and environmental impacts associated with increased material consumption. Currently,
 248 this decision-making process relies mainly on experience of individual practitioners. In
 249 fact, it can be handled analytically using a multi-objective optimization technique, i.e.,

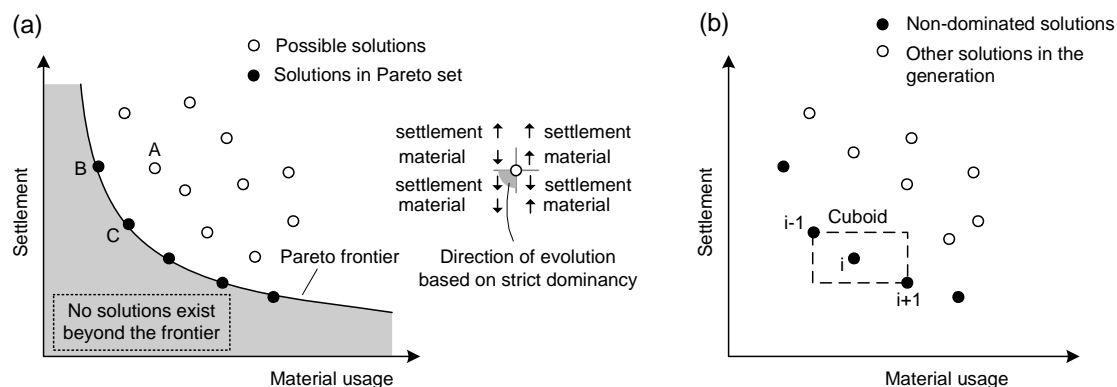


Figure 2: (a) Concept of Pareto optimality in foundation optimization; (b) Calculation of crowding distance (after Deb et al., 2002)

250 to obtain the least amount of material required to achieve a certain level of performance,
 251 meanwhile ensuring the foundation material is arranged in an optimized manner.

252 In the current study, the DE is implemented under a multi-objective optimization
 253 framework based on the concept of Pareto optimality (Fig. 2a) (Reddy and Kumar 2007;
 254 Lavan and Dargush 2009). Under this framework, a 'Pareto frontier' is defined as an
 255 optimized relationship between the objectives of optimization (e.g., foundation cost and
 256 foundation settlements) where no further improvement can be made for one criterion
 257 without worsening the other. This means, in the context of foundation optimization,
 258 that no configuration can exist 'beyond' the Pareto frontier, with both a smaller amount
 259 of material usage and a better performance compared to configurations on the frontier.

260 In multi-objective foundation optimization, the aim of DE is to obtain the Pareto
 261 frontier, which is an initially unknown relationship of optimized material usage and
 262 foundation performance. In this case, a fitter solution is defined as the one that is
 263 not worse in any objectives, and better in at least one objective, compared to another
 264 solution. This condition is known as 'strict dominancy'. As illustrated in Fig. 2a,
 265 Solution A is strictly dominated by both Solutions B and C, since both B and C have

266 at least one criterion better (smaller settlement/material usage) than A, and are not
267 worse than A in the other criterion. Solutions B and C are not strictly dominated by
268 each other, since B involves less material and C leads to smaller settlements. This is
269 also the case for all solutions on the Pareto frontier. Incorporating this concept into
270 the context of DE, a trial vector replaces another if it strictly dominates the other
271 trial vector. Consequently, an initial random population (empty circles in Fig. 2a)
272 will gradually ‘march’ towards, and eventually converge on, the Pareto frontier as they
273 evolve in subsequent generations.

274 **Elitist non-dominated sorting**

275 In typical ‘single-objective’ evolutionary algorithms, a ‘child’ vector is only compared
276 with its own ‘parent’ vector (i.e. \mathbf{y}_i with \mathbf{x}_i at the same i). Consequently, some good
277 solutions may be lost in the process if they are better than many other solutions but
278 weaker than its own parent. This issue is more prominent in multi-objective optimiza-
279 tion problems, as \mathbf{y}_i can be strong in one criterion but is eventually discarded for being
280 slightly weaker than \mathbf{x}_i in another criterion. To preserve these ‘good’ solutions and
281 hence speed up the optimization process, the idea of the non-dominated elitist archive
282 (Deb et al. 2002; Reddy and Kumar 2007) is adopted in the current study. This archive
283 is essentially a list of the best non-dominated solutions in the current generation, and al-
284 lows comparisons among all the trial vectors (i.e. all \mathbf{y}_i and \mathbf{x}_i where $i = 1, 2, \dots, NP$) in
285 the previous and current generations. The process may be interpreted as the evolution
286 of the entire frontier, instead of individual candidates, in each generation.

287 In addition, due to the random nature of DE, the resulting Pareto set may lack
288 a desirable spread of solutions along the frontier, with solutions being ‘crowded’ in
289 some regions but few and far between in others. To obtain a good spread of solutions
290 in the generation, a ‘crowding distance’ is evaluated for each solution in the archive

291 generation (Fig. 2b) (Deb et al. 2002). The crowding distance of solution i is defined
292 as the average side length of the cuboid formed by the two adjacent solutions ($i - 1$
293 and $i + 1$). In case the size of the non-dominant archive becomes bigger than the
294 population size, the final population will be decided based on the crowding distance
295 of each individual solution, and those with a large crowding distance are preferred.
296 This helps to enhance representation of the Pareto set and improve the efficiency of
297 multi-objective optimization.

298 **Case study of Hyde Park Cavalry Barracks, London**

299 The Hyde Park Cavalry Barracks (HPCB) Tower in London, U.K., will be used to
300 evaluate the coupled superstructure-foundation analysis approach, and to illustrate the
301 capabilities of the optimization technique. The foundation geometry, underlying soil
302 conditions, instrumentation setup and back analyses for the piled raft foundation have
303 been reported extensively by Hooper (1973, 1979). In addition, superstructure plans
304 and section sizes have been described in detail. Such information enables the modeling
305 of the foundation, taking into account the effects of superstructure stiffness.

306 **Details of superstructure, foundation and soil properties**

307 The HPCB tower is 90 m tall with a two-storey basement. The tower is founded on a
308 1.52-m thick raft supported by 51 under-reamed piles, each with a length of 24.8 m, shaft
309 diameter of 0.91 m and base diameter of 2.44 m. Fig. 3a shows the actual foundation
310 layout, where the shaded area represents the plan area of the raft that is in contact with
311 the soil. The subsurface soil profile consists of 5 m of fill, sand and gravel, followed by a
312 58-m thick layer of London Clay. The London Clay is underlain by the Lambeth Group
313 with a thickness of approximately 21 m, which is in turn underlain by a thin layer of
314 Thanet sand and Chalk bedrock. The groundwater level was approximately 4 m below

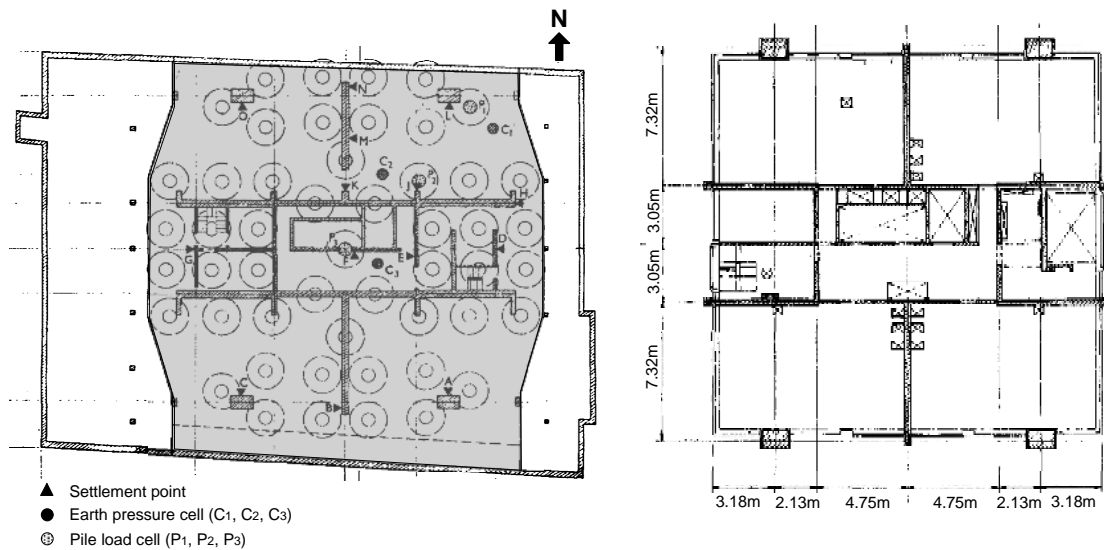


Figure 3: Foundation and superstructure layout of Hyde Park Cavalry Barracks (Hooper 1973)

315 the ground surface. For modeling purposes, it is assumed in the subsequent analyses
 316 that properties of the Lambeth Group are not significantly different from those of the
 317 London Clay.

318 The concrete tower consists of 31 storeys and the typical structural floor plan is
 319 shown in Fig. 3b. The thicknesses of core walls are 381 mm and 457 mm up to the
 320 second floor, 229 mm and 381 mm between the third and ninth floors, and 229 mm and
 321 305 mm on and above the tenth floor. The floor slabs are 178 mm thick, supported
 322 on the inner side by the core walls, and on the outer side by edge beams that are
 323 1070 mm deep and 152 mm thick. The main tower columns are 1520 mm by 915 mm.
 324 The top floor and roof are believed to have a different layout. Their exact layout is,
 325 however, not reported in the literature and therefore the floor plans are assumed to be
 326 constant throughout. Sensitivity analyses have been conducted by varying the layout
 327 and section sizes of the top two floors, and they only have a minimal impact on the
 328 overall foundation behavior.

329 The properties of London Clay are essential for foundation modeling as the piled

330 raft is entirely embedded in this type of soil. Based on the soil test data reported in
 331 Hooper (1973), Eq. (8) is derived to represent the increase of undrained shear strength
 332 (in kPa) with depth (in metres):

$$s_u = 100 + 11z_{clay} \quad (8)$$

333 where z_{clay} is the depth measured from top of the clay surface, which is approximately
 334 5 m below ground surface. The pile shaft resistance was estimated using the total
 335 stress approach (α -method), adopting $\alpha = 0.5$. The shaft resistance estimated by the
 336 total stress method and the effective stress method (assuming typical London Clay
 337 parameters) are similar to each other, and the α -method is adopted as it is based on *in-*
 338 *situ* measurements of s_u . Meanwhile, based on previously published data and results of
 339 back-analyses, Hooper (1973) proposed the following relationship between the drained
 340 and undrained Young's moduli (E' and E_u) of the London Clay (in MPa) and the
 341 corresponding depth:

$$E' = 0.75E_u = 0.75(10 + 5.2z) \quad (9)$$

342 where z is the depth (in metres) measured from the ground surface. The factor 0.75
 343 corresponds to a drained Poisson's ratio of 0.1. The shear modulus can then be esti-
 344 mated for evaluation of interaction effects between the soil, pile and raft elements (\mathbf{K}^*
 345 and λ^* in Eq. (5)), using the Chan et al. (1974) solution with Chalk layer taken as the
 346 firm stratum.

347 **Validation of piled raft analysis incorporating superstructure stiffness**

348 Hooper (1973) adopted an 'equivalent raft thickness' (t_e) of 3.3 m in his back analyses to
 349 simulate the stiffening effects of the superstructure. This is more than 100% larger than
 350 the actual thickness of the raft (1.52 m). In the current study, the matrix condensation

351 method is applied for more realistic foundation analyses and subsequent optimization.
352 The superstructure is modelled using LUSAS, which is a commercial finite element
353 software package. The condensed structural matrix (\mathbf{K}^s) is then obtained through
354 procedures described earlier (Fig. 1), assuming a long-term concrete Young's modulus
355 of 14 GPa, which takes into consideration the creep behavior of concrete. The value of
356 long-term concrete modulus is recommended by the LUSAS program, and agrees with
357 the estimates based on Eurocode 2 (British Standards Institution 2008).

358 According to Hooper (1973), the estimated total weight of the structure, including
359 dead and live loads, is 228 MN, which matches the estimates from the structural finite
360 element model when gravity loads of 3 kPa (including live loads and floor finishes)
361 are applied on all the floor slabs. Line loads of 2 kN/m are imposed on the outer
362 edge beams to simulate the weight of the façade including precast concrete elements
363 and window panes. The column and wall reactions (\mathbf{p}^w) arising from these loads are
364 applied as downward vertical loads, while the unloading due to excavation for basement
365 construction, minus the weight of the foundation raft, is applied as an uplift pressure.

366 Fig. 4a shows an encouraging agreement between measured settlements and analyses
367 with \mathbf{K}^s incorporated. The settlement at the raft center is predicted to be 23.5 mm by
368 the analyses, while the measured center settlement was 21 mm. The estimated differen-
369 tial settlements range from 5–6.5 mm in various directions, while the measured values
370 were between 3.5–6.5 mm. On the other hand, analyses without considering superstruc-
371 ture effects overestimate the differential settlements of the foundation (>10 mm), in
372 some cases by more than 100%. This would lead to overestimating the distortion and
373 potential cracking in the structure, or may lead the designers to adopt unnecessarily
374 thick rafts resulting in increases in material use and cost. For example, the equivalent
375 raft thickness ($t_e = 3.3$ m) adopted by Hooper (1973) was based on two-dimensional,
376 axisymmetric finite element analyses, to represent a tenfold increase in raft bending stiff-

Table 1: Comparisons between results of staged and ‘instantaneous’ construction models of HPCB tower

	Staged construction	‘Instantaneous’ construction
Center settlement (mm)	23.3	23.4
Differential settlement (N-S)(mm)	5.1	5.1
Differential settlement (E-W)(mm)	5.2	5.2
Differential settlement (diagonal)(mm)	6.7	6.6
Maximum differential settlement (mm)	14.6	14.5

ness compared to the actual raft thickness. Alternatively, using the piled raft analysis model in this study, sensitivity analyses are performed by increasing the raft thickness without incorporating \mathbf{K}^s . Fig. 4b shows the results of this sensitivity study, where the settlement measurements can be matched by adopting t_e of 2 m. This represents a 32% increase compared to the actual raft thickness.

The previous analyses are performed with the assumption that the complete superstructure stiffness and loads are imposed onto the foundation ‘instantaneously’. To investigate the effects of progressive loading on foundation settlements described by Brown and Yu (1986), a stepwise analysis was also performed where three construction stages are considered – at 10 storeys, 20 storeys, and completion of building. For each stage, the corresponding structure models are constructed to obtain the associated \mathbf{K}^s matrix and \mathbf{p}^w vector, and the incremental displacements (\mathbf{u} and \mathbf{u}^{ip}) are then solved according to Eq. (5). Table 1 compares the final settlement estimates from the ‘instantaneous’ and ‘staged’ load assumptions, and shows that the settlement values are almost identical. To reduce computational effort, the subsequent optimization analyses are therefore performed with the assumption of instantaneous loading as the main selection criterion is the differential settlements in the foundation.

Fig. 5 shows the comparison between the measured pile loads and predictions by

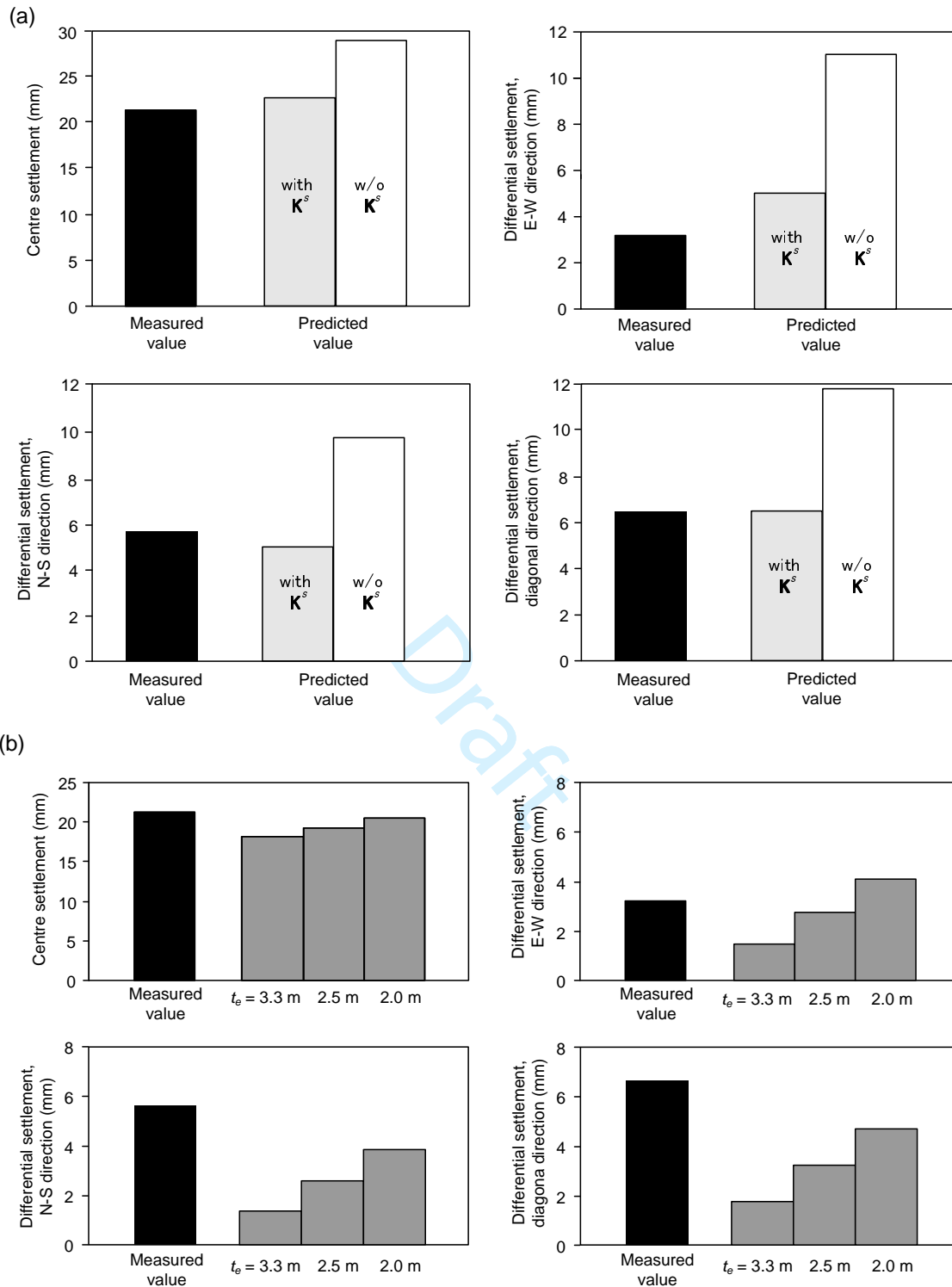


Figure 4: (a) Comparisons of settlement estimates for Hyde Park Cavalry Barracks; (b) Sensitivity analyses with different equivalent raft thickness (K^s not incorporated)

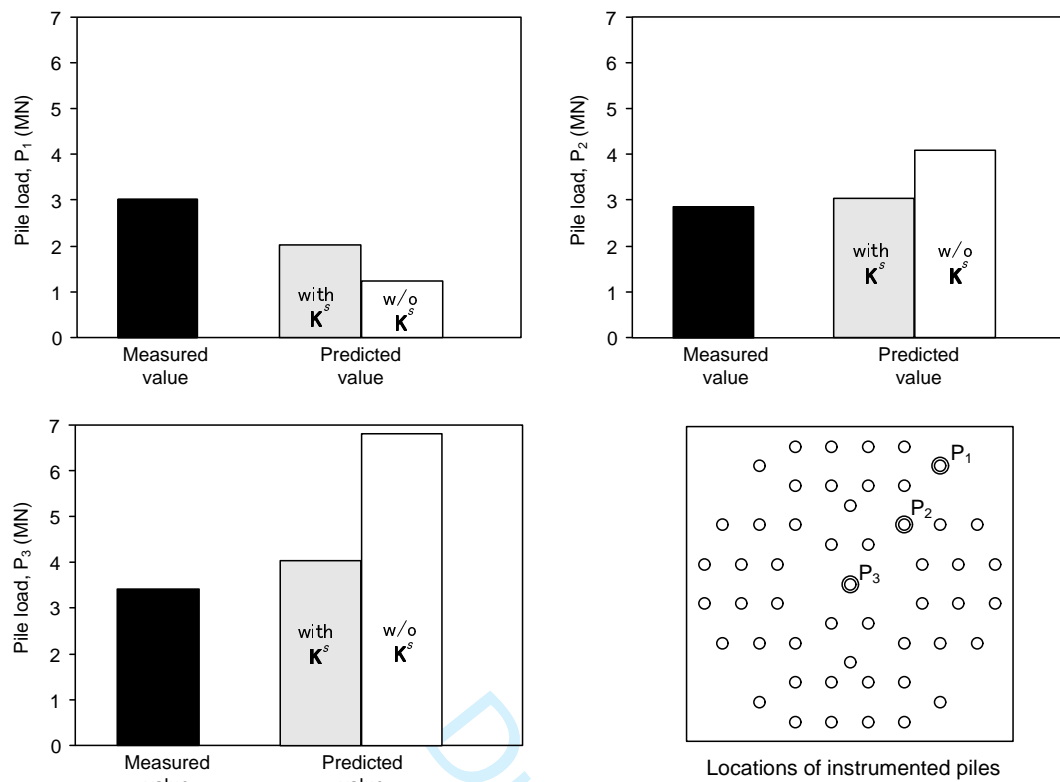


Figure 5: Comparisons of pile force estimates for Hyde Park Cavalry Barracks

395 the current analyses. Pile force estimates (incorporating K^s) for piles P1, P2 and
 396 P3 range from about 2000 kN to 4100 kN, while the measured forces were between
 397 2850 kN to 3400 kN. The maximum discrepancy between the estimated and measured
 398 values is approximately 30% (pile P1). On the other hand, without including K^s , the
 399 discrepancies for pile force estimates range from 44% to over 100% for the three piles.
 400 The improvements obtained through incorporating K^s are significant, as the building
 401 stiffness also affects the distribution of loads onto the foundation system.

402 Optimization of HPCB foundation

403 The case study of HPCB foundation can also be used to illustrate the multi-objective
 404 optimization approach, with K^s incorporated into the foundation analyses. Coding the
 405 foundation configuration as trial vectors is a key aspect in DE. This is shown in Fig. 6,

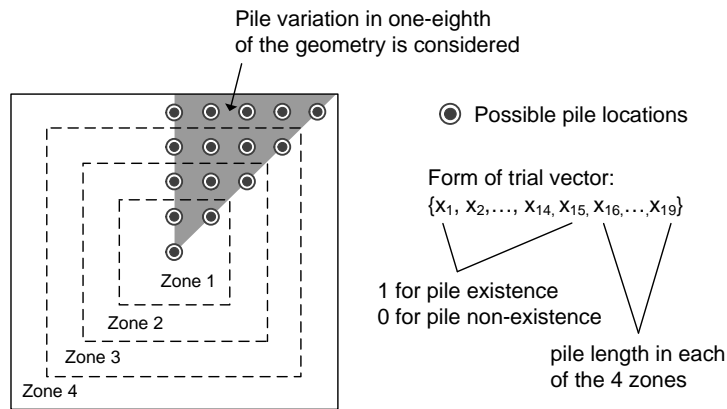


Figure 6: Optimization scheme for piled raft of Hyde Park Cavalry Barracks

406 which outlines the scheme to optimize both the pile lengths and pile locations for the
 407 HPCB piled raft. The scheme takes advantage of piled raft symmetry and imposes
 408 uniform pile lengths at similar distances from the center. As illustrated by the shaded
 409 area in Fig. 6, a trial vector represents the variations of pile geometry in one-eighth of
 410 the foundation geometry, and the variations are imposed to the entire foundation to
 411 ensure symmetric conditions. For the HPCB foundation, the trial vector consists of 15
 412 possible pile locations. Each of the first 15 components (position components) of the
 413 trial vector is equal to either 1 or 0, and determines the existence or non-existence of
 414 piles in each of the 15 locations. The second part of the vector (length components),
 415 consisting of 4 components in this case, controls the pile lengths in each of the 4 zones at
 416 different distances from the center of the raft. The length of trial vector, D , is therefore
 417 19 in this case.

418 In the current study, the selection criterion in the DE algorithm is to minimize
 419 the differential settlement, defined herein as the difference between the maximum and
 420 minimum settlements across the raft. Depending on specific project conditions, other
 421 criteria may be applicable. Examples of these could include the rocking movements
 422 and horizontal deflections due to wind loads on very tall buildings, which will result

423 in different optimized pile configurations. The purpose of the following analyses is
424 to demonstrate the capabilities of the proposed technique under a certain selection
425 criterion, which is the differential settlement under vertical loads.

426 To ensure realistic pile configurations in the optimization, the numbers of piles are
427 allowed to vary between 45 to 55, and the maximum ratio between the longest and
428 shortest pile lengths is 1.5. The pile diameter is assigned to be 0.91 m, which is the
429 same as the original configuration. Optimization analysis is then performed with a
430 population size (NP) of 100.

431 Multi-objective optimization places a high demand on computing power due to the
432 large number of possible pile configurations with varying amounts of material. There-
433 fore, a two-stage optimization approach has been adopted. The Pareto frontier is first
434 developed using linear-elastic piled raft analyses, where the large number of potential
435 pile configurations is evaluated using relatively fast elastic analyses. In the second
436 stage, the frontier is refined by subjecting the solutions on the ‘elastic’ frontier to more
437 rigorous elastic-plastic analyses.

438 Fig. 7 shows the Pareto frontier developed by this two-stage optimization approach.
439 Fig. 7a shows the first stage using the elastic analyses, whereas the solid circles in
440 Fig. 7b are the Pareto frontier refined by the second stage, using elastic-plastic anal-
441 yses. The process of evolution towards the frontier is revealed by the distribution of
442 solutions in the 10th, 20th and 50th generations, as shown in Fig. 7a. The analysis is
443 terminated at the 50th generation as a stable frontier has developed, and the resulting
444 configurations are subjected to elastic-plastic analyses, leading to the refined frontier
445 shown in Fig. 7b (solid circles). Average settlements of several configurations on the
446 frontier are also shown in Fig. 7b as they can be important concerns in the design. For
447 verification purposes, optimization with elastic-plastic analyses, which should result in
448 the true frontier, is also performed for comparison, using a smaller NP of 30 to reduce

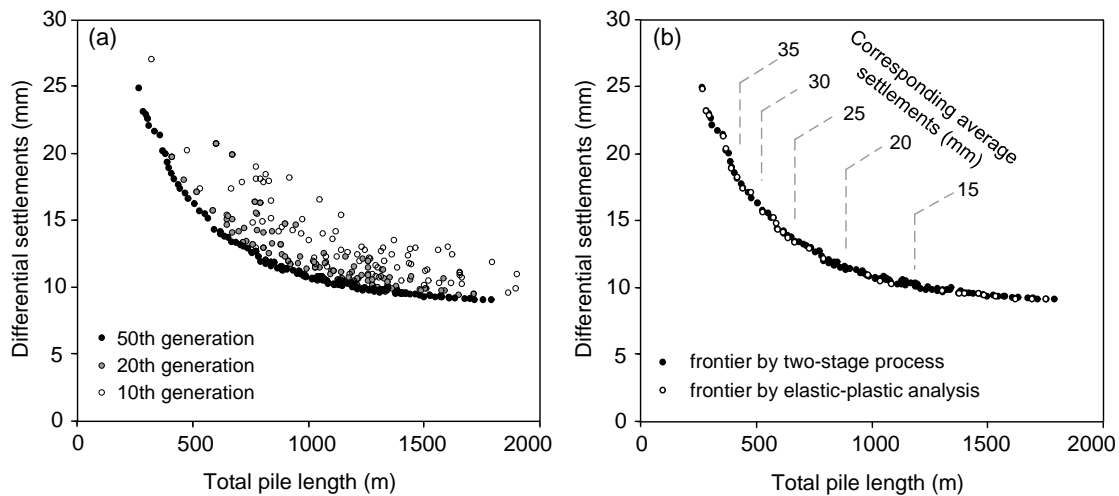


Figure 7: (a) Development of Pareto frontier using the two stage process; (b) Refined Pareto frontier with elastic-plastic analyses

449 the required computational effort. This frontier is shown by empty circles in Fig. 7b.
 450 Not only do the two frontiers coincide with each other, the geometries of optimized
 451 configurations obtained from the two sets of analyses are also very similar.

452 The two-stage process involves optimization using elastic analyses, refined by elastic-
 453 plastic analyses on the final Pareto set. In theory, the frontier developed by elastic
 454 analyses (Stage 1) is the lower bound of the true relationship since elastic analyses
 455 always result in displacements smaller than or equal to those predicted by nonlinear
 456 analyses. On the other hand, the refined frontier developed at Stage 2 represents the
 457 upper bound of the true frontier. This is because if the true frontier consists of ‘fitter’
 458 configurations than the refined frontier, they must result in smaller displacements than
 459 those in the two-stage process. In the case of HPCB Tower foundation, the frontier
 460 developed by the two-stage process (Fig. 7a) is almost identical to the refined frontier
 461 (Fig. 7b). This is mainly because the raft alone provides sufficient resistance to resist the
 462 structural loads, while the piles are installed mainly to control settlements. The overall
 463 margin of capacity provided by the piled raft is large - hence the degree of nonlinearity

464 is low - resulting in similar predictions of displacements by elastic and elastic-plastic
465 analyses.

466 **Discussions on optimized pile configurations**

467 The Pareto frontier entails optimized pile configurations with different amounts of mate-
468 rial usage, represented in this case by the sum of lengths (or total lengths) of all piles in
469 the piled raft. A closer examination of these configurations reveals that they share simi-
470 lar general characteristics. For example, Fig. 8 shows the optimized configurations with
471 total lengths of all piles being 500 m (Fig. 8a), 1250 m (Fig. 8b) and 1500 m (Fig. 8c).
472 All these configurations consist of piles directly underneath the heavily-loaded shear
473 walls of the tower (Fig. 3). In general, longer piles are located close to the central
474 part of the raft while shorter piles are placed near the periphery to reduce differential
475 settlements. The features of these configurations also match with the general recom-
476 mendations by Leung et al. (2010b) and Reul and Randolph (2004), who stated that
477 considering the same total pile length, using small numbers of long piles is more effective
478 in reducing settlements, and differential settlements are efficiently reduced by installing
479 piles under the central area of the foundation.

480 The original pile configuration (Fig. 3) involves a total pile length of about 1250 m,
481 resulting in differential settlement of 14.5 mm. According to Fig. 8b, the optimized
482 layout with 1250 m of pile material results in differential settlement of only 10 mm,
483 which represents a 30% reduction. On the other hand, for a required performance level
484 of 14.5 mm in differential settlements, it is possible to reduce the total pile material
485 to 650 m according to the Pareto frontier (Fig. 7), which represents a reduction of
486 approximately 50% in pile material.

487 Apart from foundation settlements, the pile forces and bending moments induced
488 in the raft are also evaluated by the proposed approach. Fig. 9 compares bending mo-

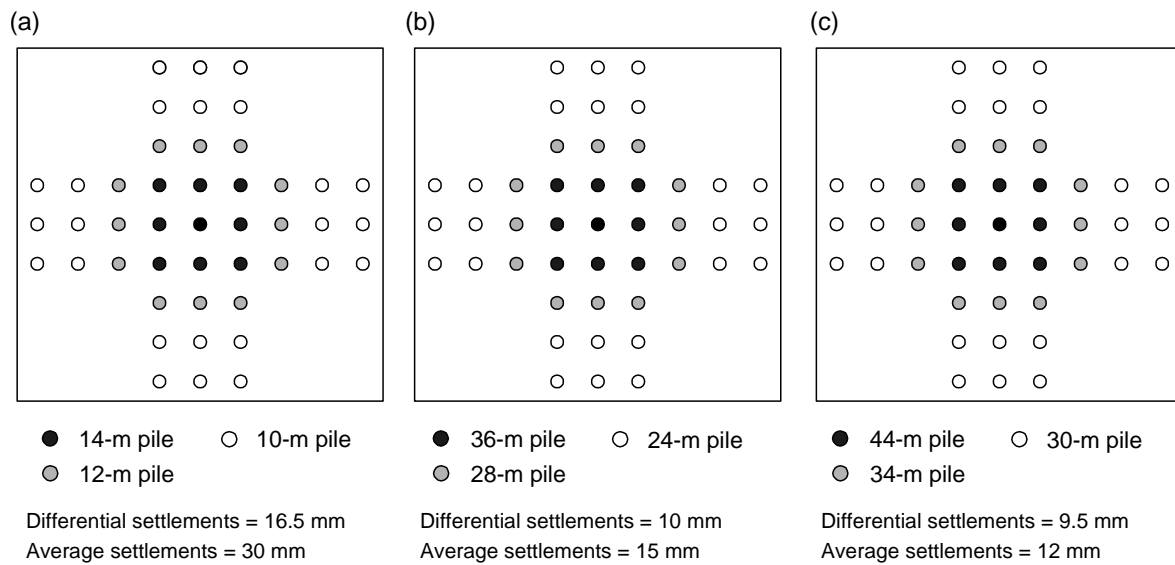


Figure 8: Optimized pile configurations with different total pile lengths of (a) 500 m; (b) 1250 m; (c) 1500 m. Original configuration involves total pile length of 1250 m, average settlement of 17 mm and differential settlement of 14.5 mm

489 ments evaluated based on the original pile configuration (Fig. 3a) and the optimized
 490 configuration, with total pile length of 1250 m (Fig. 8b). Under the optimized configura-
 491 tion, the bending moments are reduced in the central area of the raft, but there are
 492 slight increases near the raft edges, as it consists of fewer piles near the edge columns
 493 of the structure than the original configuration.

494 Fig. 10 compares the maximum and minimum pile forces in the original and opti-
 495 mized piled raft configurations (Fig. 8b), and shows that the range of pile force variation
 496 has not been significantly altered in the optimized configuration. In the current opti-
 497 mization scheme, the maximum ratio between the longest and shortest pile lengths is
 498 1.5. The rationale behind this limit is to avoid ‘ultra-long’ piles in the foundation,
 499 which tend to attract more load than other piles, and where defects or underperfor-
 500 mance of such elements can be more detrimental. Over-reliance on certain long piles
 501 can undermine the redundancy of a foundation system as the overall reliability hinges
 502 on the behavior of a few very stiff elements. The maximum/minimum pile length ratio

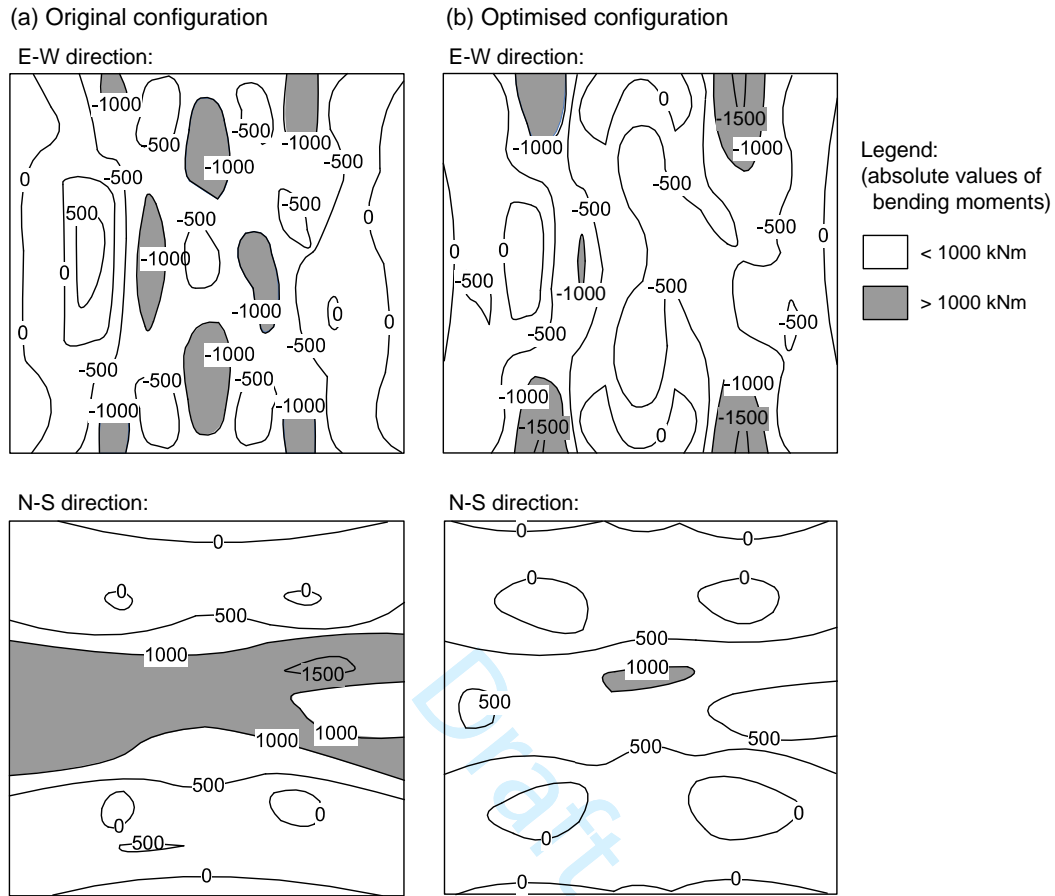


Figure 9: Bending moment estimates for (a) original pile configuration and (b) optimized pile configuration with total pile length of 1250 m

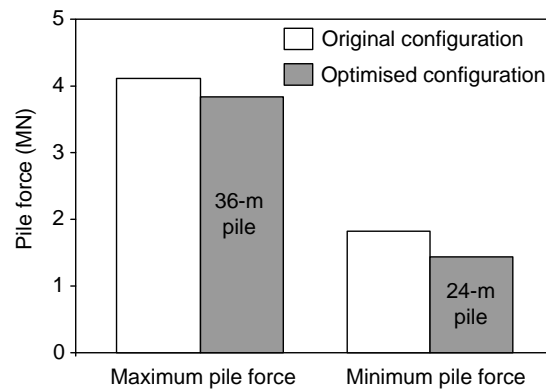


Figure 10: Comparisons of maximum and minimum pile forces between original and optimized pile configurations for HPCB tower

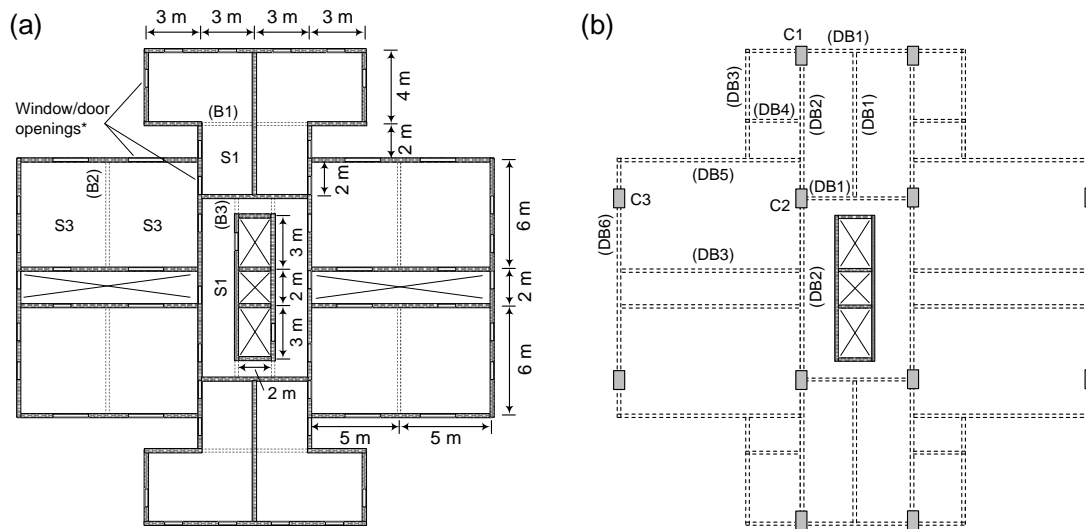
503 of 1.5 helps to ensure redundancy in the foundation design is not compromised in the
504 optimized configuration.

505 **Case study of building with soft storey on ground floor**

506 The HPCB building consists of floor layouts that remain relatively constant throughout
507 the height of the building, although the shear wall thickness varies slightly on different
508 storeys. However, in order to create open space on the ground floor, it is not uncommon
509 for buildings to incorporate an atrium floor that is significantly less stiff than the upper
510 storeys. This abrupt change in floor layout may influence how the superstructure
511 stiffness is transferred to the foundation system.

512 Fig. 11 shows the floor plans simplified from a typical residential block in Hong
513 Kong, China, which is a 25-storey reinforced concrete building with an atrium on the
514 ground floor and 24 typical upper floors. The atrium floor consists of 12 columns with
515 dimensions ranging from 762 mm × 1219 mm to 762 mm × 1829 mm. From the second
516 storey upward, the floor layout consists of concrete walls with thickness of 152 mm.
517 Apart from the 4-m high atrium, each storey is 3 m in height, with floor slab thickness
518 varying from 102 mm to 127 mm in different areas of each floor. The atrium and upper
519 floors are connected by deep transfer beams with section sizes ranging from 381 mm
520 × 1219 mm (width × depth) to 889 mm × 2565 mm. To illustrate the significance of
521 the open atrium, a second building model is created without the atrium for comparison
522 purposes. This building consists of 25 storeys of the same floor plan as shown in Fig. 11a.
523 The first storey is 4 m high while the upper floors are all 3 m in height. Besides the
524 self weights of structural components, 5 kPa of superimposed dead load and live loads
525 are modelled, and the \mathbf{K}^s matrix and \mathbf{p}^w vector for each building are obtained using
526 the procedures described earlier.

527 The two buildings are assumed to be founded on piled rafts, and the soil condi-



Dimensions of slabs (S), beams (B, DB) and columns (C):

S1: 102 mm (thickness)	B1: 152 mm x 457 mm	C1: 762 mm x 1219 mm	DB1: 610 mm x 2565 mm
S2: 114 mm (thickness)	B2: 305 mm x 457 mm	C2: 762 mm x 1829 mm	DB2: 762 mm x 2565 mm
S3: 127 mm (thickness)	B3: 152 mm x 381 mm	C3: 889 mm x 1295 mm	DB3: 457 mm x 2565 mm
			DB4: 381 mm x 1219 mm
			DB5: 686 mm x 2565 mm
			DB6: 889 mm x 2565 mm

*Windows are modelled as 1 m x 1 m or 2 m x 1 m openings, while doors are modelled as 2 m x 1 m openings

Figure 11: Superstructure layout for hypothetical building: (a) typical floor; (b) atrium floor. Building is symmetrical in two directions

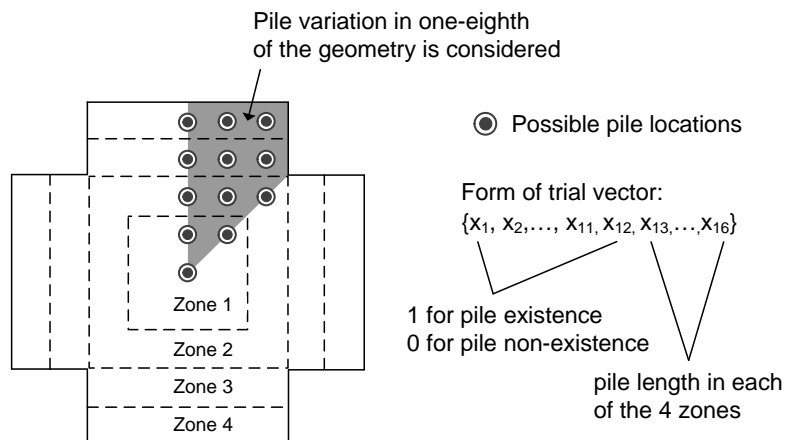


Figure 12: Optimization scheme for piled raft of hypothetical building

528 tions for this hypothetical case consist of a homogeneous soil layer with $E' = 40$ MPa
529 and Poisson's ratio of 0.3. The pile capacities are evaluated using the effective stress
530 approach, assuming a friction angle of 32° and shaft resistance coefficient of 0.5. The
531 water table is assumed to be at the base of a 1.5-m thick raft.

532 As shown in Fig. 12, the raft is modelled with a cruciform shape to match the
533 superstructure layout, while the pile optimization scheme is derived to take advantage
534 of the symmetry conditions. The trial vector consists of 16 components, where the first
535 12 determine pile locations and the remaining 4 decide the pile lengths at various zones.
536 The pile diameter is taken as 0.9 m, the number of piles is allowed to vary from 40 to
537 55, and the maximum length ratio is 1.5 as in the HPCB case.

538 **Influence of atrium floor on foundation optimization**

539 Multi-objective optimization analyses are performed for the two buildings, one with
540 the atrium design at ground floor level and the other one with constant floor stiffness
541 and no atrium. For both optimization analyses, the population size (NP) is 100, and
542 the two-stage approach is adopted with Pareto frontiers first developed using linear-
543 elastic analyses, and then refined by elastic-plastic analyses. Fig. 13a shows the Pareto
544 frontiers for the optimized piled raft foundations supporting the two different buildings.
545 Although the two superstructures only differ by the first storey, the difference in the
546 performance of the optimized foundations is notable. For example, with the material
547 usage of approximately 400 m in total pile length, the optimized pile configuration leads
548 to differential settlements of 6 mm for the building with an atrium, and only about 3 mm
549 for the building with shear walls on the first storey and no atrium. In other words, the
550 presence of an atrium floor reduces the stiffening effects of the superstructure, as the
551 stiffness of shear walls on upper storeys is not effectively transferred to the foundation.

552 Considering the same pile configurations, Fig. 13a also shows the corresponding anal-

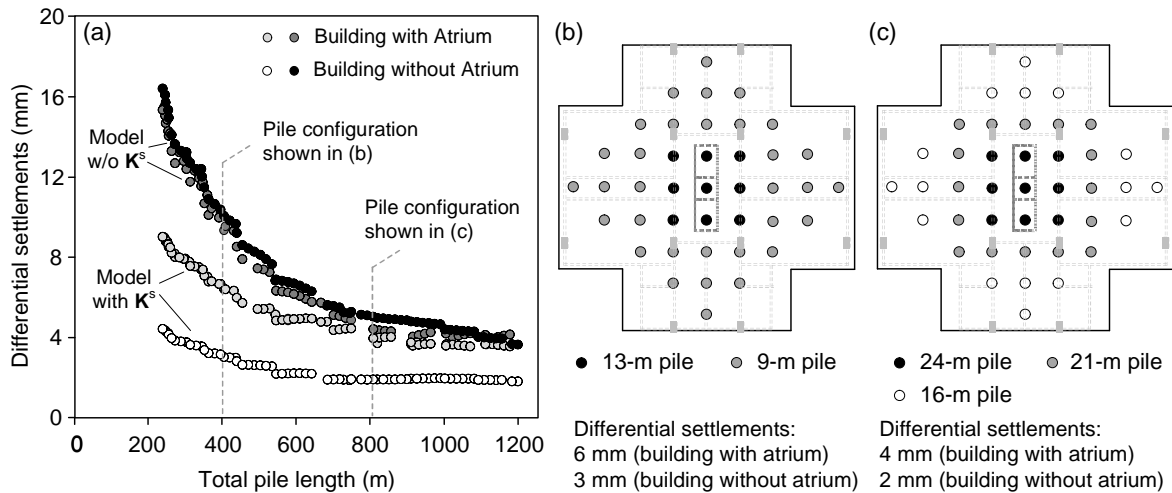


Figure 13: Pareto frontiers and optimized pile configurations for buildings with and without atrium floor

553 uses when the superstructure stiffness (K^s) is not coupled with the foundation model.
 554 For both cases, the differential settlements are larger when K^s is not considered. As
 555 the superstructure and foundation behave in a holistic manner, the importance of K^s
 556 also depends on the stiffness of the foundation system. The stiffening effects of the
 557 superstructure are more substantial when small amounts of pile material are used, and
 558 gradually diminishes as the pile length increases, i.e., when stiffer foundations are in-
 559 stalled. In most cases, however, the influence of K^s should not be overlooked. For
 560 example, with the building geometry shown in Fig. 11, differential settlements of about
 561 13 mm correspond to a deflection ratio of 0.05%. If this is adopted as the allowable limit
 562 for the structure, analyses without including K^s could lead the engineer to increase the
 563 number of piles or the thickness of raft in the foundation design. This again highlights
 564 the importance of realistic modeling of superstructure-foundation interactions for pile
 565 group/piled raft analysis and optimization. Two examples of the optimized pile confi-
 566 gurations are shown in Figs. 13b and c. Although optimization analyses are performed
 567 separately for the two buildings, the resulting optimized pile configurations are iden-

568 tical at most cases of material usage. This may be attributed to the fact that load
569 distributions across the foundations are similar between the two buildings. The 24 typ-
570 ical upper storeys involve the same floor layout and load patterns for both buildings.
571 Although such loadings are carried by columns at the atrium floor, and by walls for
572 the building without the atrium, they eventually lead to similar load distribution on
573 the raft and hence the same optimized pile configurations. Similar to the HPCB case,
574 the optimized configurations involve long piles near the center of the foundation and
575 shorter piles around the periphery, which is typical when the optimization criterion
576 involves minimizing differential settlements under vertical loads.

577 **Conclusion**

578 This paper introduces the matrix condensation method which allows coupling of su-
579 perstructure stiffness into pile group and piled raft foundation models. This approach
580 forms a link between the structural and geotechnical engineers, through which accu-
581 rate global solutions can be obtained without the need for relaxing assumptions on the
582 contribution of superstructure to the foundation system, and vice-versa.

583 Considerations of the superstructure stiffness and load distribution can play an
584 important role in the foundation optimization process, especially when structural ele-
585 ments such as shear walls contribute significantly to the settlement response of piled
586 foundations. In the current study, the coupled analysis approach is incorporated into
587 a multi-objective pile optimization algorithm, which provides a series of design options
588 at various levels of material consumption, with each design option representing the op-
589 timized configuration using that particular amount of pile material. This reveals the
590 trade-off between material usage and foundation performance, and can help engineers
591 make informed decisions on the design based on its cost-effectiveness and the perfor-
592 mance requirements. While many engineers currently rely on experience in the design

593 of pile groups, the proposed approach represents a tool that can provide added-value for
594 performance-based design and resource management, as it is very difficult, if possible at
595 all, to develop the Pareto front based on one's experience or intuition. These potential
596 benefits can easily outweigh the additional analysis efforts with increasing complexity
597 in project constraints and performance requirements.

598 The coupled superstructure-foundation analysis approach is validated against mea-
599 surements of a piled raft-supported building in London, U.K., where the superstructure
600 layout and original pile configuration are closely modelled. Optimization analyses are
601 then performed, and show that with the same amount of pile material, the differential
602 settlements can be reduced by 30% by adopting the optimized pile layout. On the other
603 hand, to achieve a performance level (differential settlements) similar to the original
604 design, the required pile length can be reduced by 50% if an optimized layout is adopted
605 in lieu of the original configuration.

606 A second case study is then presented to illustrate the effects of having a soft storey
607 (atrium floor) on the superstructure-foundation interactions. Although the two build-
608 ings in this case only differ by the atrium floor, the resulting difference in terms of
609 superstructure stiffness is notable. Considering the specific loading and foundation con-
610 ditions, the differential settlements for the building with the atrium is approximately
611 2 times that of the building with shear walls on ground floor. This shows that stiff-
612 ness of the upper storeys may not be effectively transferred to the foundation system
613 when a soft storey is present. Nonetheless, this study has shown that for various cases
614 of high-rise buildings with significant amounts of shear walls, the stiffening effects of
615 the superstructure can be important and should be carefully considered in foundation
616 analysis and optimization strategies.

617 **Acknowledgements**

618 The work presented in this paper is financially supported by the Engineering and Physi-
619 cal Sciences Research Council of the United Kingdom (Project No. EP/D040000/1), and
620 the Research Grants Council of the Hong Kong Special Administrative Region (Project
621 No. 15220415). The finite element models for the second case were constructed by
622 Mr. Zhenxiang Su of The Hong Kong Polytechnic University. His efforts are gratefully
623 acknowledged.

Draft

References

- British Standards Institution 2008. *Eurocode 2: Design of concrete structures — Part 1-1: General rules and rules for buildings*. BSI, London, BS EN 1992-1-1:2004.
- Brown, P. T. and Yu, S. K. R. 1986. “Load sequence and structure-foundation interaction.” *Journal of Structural Engineering*, 112(3), 481–488.
- Chamecki, S. 1956. “Structural rigidity in calculating settlements.” *Journal of the Soil Mechanics and Foundation Division*, 82(SM1), 1–19.
- Chan, C. M., Zhang, L. M., and Ng, J. T. M. 2009. “Optimization of pile groups using hybrid genetic algorithms.” *Journal of Geotechnical and Geoenvironmental Engineering, ASCE*, 135(4), 497–505.
- Chan, K. S., Karasudhi, P., and Lee, S. L. 1974. “Force at a point in the interior of a layered elastic half space.” *International Journal of Solids Structures*, 10, 1179–1199.
- Chow, Y. K. and Thevendran, V. 1987. “Optimisation of pile groups.” *Computers and Geotechnics*, 4, 43–58.
- Comodromos, E. M., Papadopoulou, M. C., and Laloui, L. 2016. “Contribution to the design methodologies of piled raft foundations under combined loadings.” *Canadian Geotechnical Journal*, 53, 559–577.
- Deb, K., Pratap, A., Agarwal, S., and Meyarivan, T. 2002. “A fast and elitist multi-objective genetic algorithm: NSGA-II.” *IEEE Transactions on Evolutionary Computation*, 6(2), 182–197.
- Guo, W. D. and Randolph, M. F. 1997. “Vertically loaded piles in non-homogeneous media.” *International Journal for Numerical and Analytical Methods in Geomechanics*, 21, 507–532.
- Hooper, J. A. 1973. “Observations on the behaviour of a piled-raft foundation on London clay.” *Proceedings of the Institution of Civil Engineers*, 55, 855–877.

- Hooper, J. A. 1979. *Review of behaviour of piled raft foundations*. CIRIA Report No. 83, Construction Industry Research and Information Association, London.
- Horikoshi, K. and Randolph, M. F. 1998. "A contribution to optimum design of piled rafts." *Géotechnique*, 48(3), 301–317.
- Hwang, J., Lyu, Y., and Chung, M. 2011. "Optimizing pile group design using a real genetic approach." *Proceedings of the International Offshore and Polar Engineering Conference*, 491–499.
- Katzenbach, R., Arslan, U., and Moormann, C. 2000. "Piled raft foundation projects in Germany." *Design applications of raft foundations*, J. A. Hemsley, ed., Thomas Telford, 323–391.
- Kim, H. T., Yoo, H. K., and Kang, I. K. 2002. "Genetic algorithm-based optimum design of piled raft foundations with model tests." *Journal of the Southeast Asian Geotechnical Society*, 33(1), 1–11.
- Kim, K. N., Lee, S.-H., Kim, K.-S., Chung, C.-K., Kim, M. M., and Lee, H. S. 2001. "Optimal pile arrangement for minimizing differential settlements in piled raft foundations." *Computers and Geotechnics*, 28(4), 235 – 253.
- Klar, A., Vorster, T. E. B., Soga, K., and Mair, R. J. 2007. "Elastoplastic solution for soil-pipe-tunnel interaction." *Journal of Geotechnical and Geoenvironmental Engineering, ASCE*, 133(7), 782–792.
- Lavan, O. and Dargush, G. F. 2009. "Multi-objective evolutionary seismic design with passive energy dissipation systems." *Journal of Earthquake Engineering*, 13(6), 758–790.
- Leung, Y. F. 2010. "Foundation optimisation and its application to pile reuse." Ph.D. thesis, University of Cambridge, United Kingdom.
- Leung, Y. F., Hout, N. A., Klar, A., and Soga, K. 2010a. "Coupled foundation-

- superstructure analysis and influence of building stiffness on foundation response.” *Deep Foundations and Geotechnical In Situ Testing*, 61–66.
- Leung, Y. F., Klar, A., and Soga, K. 2010b. “Theoretical study on pile length optimization of pile groups and piled rafts.” *Journal of Geotechnical and Geoenvironmental Engineering*, 136(2), 319–330.
- Leung, Y. F., Soga, K., and Klar, A. 2011. “Multi-objective foundation optimization and its application to pile reuse.” *Geo-Frontiers 2011*, 75–84.
- Leung, Y. F., Soga, K., Lehane, B. M., and Klar, A. 2010c. “Role of linear elasticity in pile group analysis and load test interpretation.” *Journal of Geotechnical and Geoenvironmental Engineering*, 136(12).
- Liu, X., Cheng, G., Wang, B., and Lin, S. 2012. “Optimum design of pile foundation by automatic grouping genetic algorithms.” *ISRN Civil Engineering*, 2012.
- Meyerhof, G. G. 1953. “Some recent foundation research and its application to design.” *The Structural Engineer*, 31, 151–167.
- Mindlin, R. D. 1936. “Force at a point in the interior of a semi-infinite solid.” *Physics*, 7, 195–202.
- Miyahara, F. and Ergatoudis, J. G. 1976. “Matrix analysis of structure-foundation.” *Journal of the Structural Division*, 102(ST1), 251–265.
- Ng, J. T. M., Chan, C. M., and Zhang, L. M. 2005. “Optimum design of pile groups in nonlinear soil using genetic algorithms.” *Proceedings of the 8th International Conference on the Application of Artificial Intelligence to Civil, Structural and Environmental Engineering*, Paper 35.
- Poulos, H. G. 1975. “Settlement analysis of structural foundation systems.” *Proceedings of the 4th Southeast Asian Conference on Soil Engineering*, Kuala Lumpur, 4–54–4–62.

- Poulos, H. G. 1979. "Settlement of single piles in nonhomogeneous soil." *Journal of the Geotechnical Engineering Division, ASCE*, 105(GT5), 627–641.
- Poulos, H. G. 1989. "Pile behaviour — theory and application." *Géotechnique*, 39(3), 365–415.
- Poulos, H. G. 2016. "Tall building foundations: design methods and applications." *Innovative Infrastructure Solutions*, 1(1), 1–51.
- Poulos, H. G., Small, J. C., Ta, L. D., Sinha, J., and Chen, L. 1997. "Comparison of some methods for analysis of piled rafts." *Proceedings of the 14th International Conference on Soil Mechanics and Foundation Engineering*, Vol. 2, Hamburg, 1119–1124.
- Reddy, M. J. and Kumar, D. N. 2007. "Multiobjective differential evolution with application to reservoir system optimization." *Journal of Computing in Civil Engineering*, 21(2), 136–146.
- Reul, O. and Randolph, M. F. 2003. "Piled rafts in overconsolidated clay: comparison of in situ measurements and numerical analyses." *Géotechnique*, 53(3), 301–315.
- Reul, O. and Randolph, M. F. 2004. "Design strategies for piled rafts subjected to nonuniform vertical loading." *Journal of Geotechnical and Geoenvironmental Engineering, ASCE*, 130(1), 1–13.
- Small, J. C. 2001. "Practical solutions to soilstructure interaction problems." *Progress in Structural Engineering and Materials*, 3(3), 305–314.
- Sommer, H. 1965. "A method for the calculation of settlements, contact pressures and bending moments in a foundation including the influence of the flexural rigidity of the superstructure." *Proceedings of the 6th International Conference on Soil Mechanics and Foundation Engineering*, Vol. 2, Montréal, 194–201.
- Storn, R. and Price, K. 1997. "Differential evolution — a simple and efficient heuris-

- tic for global optimization over continuous spaces.” *Journal of Global Optimization*, 11(4), 341–359.
- Truman, K. Z. and Hoback, A. S. 1992. “Optimization of steel piles under rigid slab foundations using optimality criteria.” *Structural Optimization*, 5, 30–36.
- Valliappan, S., Tandjiria, V., and Khalili, N. 1999. “Design of raft-pile foundation using combined optimization and finite element approach.” *International Journal for Numerical and Analytical Methods in Geomechanics*, 23, 1043–1065.
- Weigel, T. A., Ott, K. J., and Hagerty, D. J. 1989. “Load redistribution in frame with settling footings.” *Journal of Computing in Civil Engineering*, 3(1), 75–92.
- Zienkiewicz, O. C. and Taylor, R. L. 2005. *The finite element method for solid and structural mechanics*. Oxford: Butterworth-Heinemann, sixth edition.

Draft

List of Figures

1	(a) Structure condensation process using finite element simulation, considering vertical load-settlement response (Leung et al. 2010a); (b) Schematic representation of piled raft model	5
2	(a) Concept of Pareto optimality in foundation optimization; (b) Calculation of crowding distance (after Deb et al., 2002)	13
3	Foundation and superstructure layout of Hyde Park Cavalry Barracks (Hooper 1973)	16
4	(a) Comparisons of settlement estimates for Hyde Park Cavalry Barracks; (b) Sensitivity analyses with different equivalent raft thickness (\mathbf{K}^s not incorporated)	20
5	Comparisons of pile force estimates for Hyde Park Cavalry Barracks . . .	21
6	Optimization scheme for piled raft of Hyde Park Cavalry Barracks . . .	22
7	(a) Development of Pareto frontier using the two stage process; (b) Refined Pareto frontier with elastic-plastic analyses	24
8	Optimized pile configurations with different total pile lengths of (a) 500 m; (b) 1250 m; (c) 1500 m. Original configuration involves total pile length of 1250 m, average settlement of 17 mm and differential settlement of 14.5 mm	26
9	Bending moment estimates for (a) original pile configuration and (b) optimized pile configuration with total pile length of 1250 m	27
10	Comparisons of maximum and minimum pile forces between original and optimized pile configurations for HPCB tower	27
11	Superstructure layout for hypothetical building: (a) typical floor; (b) atrium floor. Building is symmetrical in two directions	29

12 Optimization scheme for piled raft of hypothetical building 29

13 Pareto frontiers and optimized pile configurations for buildings with and
without atrium floor 31

Draft